# Simulation of the inertial–conductive subrange

Jeffrey R. Chasnov
*NASA Goddard Institute for Space Studies, New York, New York 10025*

(Received 10 September 1990; accepted 5 November 1990)

The inertial–conductive subrange spectrum of a passive temperature field of a fluid of small Prandtl number is determined by large-eddy simulation. Results for simulations of both freely decaying and forced turbulence are presented. In the simulations of freely decaying turbulence, a subgrid model is used to simulate a decaying turbulent velocity field with a $k^{-5/3}$ inertial subrange energy spectrum convecting eight different decaying temperature fields with well-resolved conductive subranges. In the simulations of forced turbulence, a subgrid model is again used to simulate an inertial subrange velocity field; however, the velocity field is now forced at the lowest wave numbers of the simulation, and an external uniform mean temperature gradient is imposed. Statistically stationary velocity and temperature fluctuations are generated. The results of the decaying and forced simulations are in excellent agreement with the Batchelor, Howells, and Townsend (BHT) [J. Fluid Mech. **5**, 134 (1959)] $k^{-17/3}$ spectrum in the far inertial–conductive subrange, whereas significant departures from the BHT spectrum are observed in the near inertial–conductive subrange.

## I. INTRODUCTION

If the kinematic viscosity $\nu$ of a fluid is much less than its thermometric conductivity $\chi$, then velocity fluctuations in the fluid will persist at much smaller scales than temperature fluctuations. The scale sizes characterized by the range of wave numbers $k$ over which the velocity fluctuations are highly turbulent, but the temperature fluctuations are strongly damped by the effects of conduction, is called the inertial–conductive subrange. The determination of the correct inertial–conductive subrange spectrum of a temperature field in a fluid of small Prandtl number $\sigma = \nu/\chi$ has been a controversial problem for over 30 years. Physical experiments to investigate this subrange are difficult to perform, so that experimental data are limited, while analytical arguments abound as a result of too many dimensional quantities.

Nevertheless, the equation satisfied by a temperature field $\theta(\mathbf{x},t)$, convected by a velocity field $\mathbf{u}(\mathbf{x},t)$, is well known:

$$\frac{\partial\theta}{\partial t} + \mathbf{u}\cdot\nabla\theta = \chi\nabla^2\theta, \tag{1}$$

and, in the absence of definitive theoretical or experimental results, the remaining possibility is to solve Eq. (1) numerically for scale sizes lying in the inertial–conductive subrange.

Such numerical simulations of Eq. (1) have been recently performed by Chasnov, Canuto, and Rogallo[1] (henceforth referred to as CCR). If the temperature fluctuations do not dynamically interact with the convecting velocity field (as is typically the case when the temperature fluctuations are sufficiently small so that buoyancy effects may be ignored), the equation satisfied by $\mathbf{u}(\mathbf{x},t)$ is independent of $\theta(\mathbf{x},t)$ and the temperature fluctuations are called passive. It is then reasonable to solve Eq. (1) using a prescribed velocity field. CCR performed such a numerical simulation of the convection of a passive temperature field by a frozen Gaussian velocity field with an energy spectrum $E(k) \propto k^{-5/3}$. When the temperature fluctuations become conductive, the inertial–conductive subrange spectrum

$$G(k) = \tfrac{1}{3}\mathrm{Ko}\,\chi^{-3}\epsilon_\theta\epsilon^{2/3}k^{-17/3}, \tag{2}$$

originally proposed by Batchelor, Howells, and Townsend[2] (henceforth referred to as BHT), was recovered. The spectrum $G(k)$ is defined to yield the volume average of $\theta^2$,

$$\langle\theta^2\rangle = \int_0^\infty G(k)dk, \tag{3}$$

and $\epsilon_\theta$ is the constant flux of $\theta^2$ through wave number $k$ when conductive effects are negligible; it is also equal to the conductive dissipation rate,

$$\epsilon_\theta = 2\chi\int_0^\infty k^2 G(k)dk. \tag{4}$$

When the velocity field is prescribed, $\mathrm{Ko}\,\epsilon^{2/3}$ is the proportionality constant in front of the $k^{-5/3}$ power law of the inertial range energy spectrum

$$E(k) = \mathrm{Ko}\,\epsilon^{2/3}k^{-5/3}, \tag{5}$$

whereas, in the physical case when the velocity field is a time-evolving solution of the Navier–Stokes equation, $\epsilon$ is the constant flux of turbulent kinetic energy through wave number $k$ when viscous effects are negligible.

It should be noted that the BHT analysis does not require an inertial range energy spectrum but rather one that decays much more slowly with increasing $k$ than the temperature spectrum. In particular, the BHT result, Eq. (2), can be written in the form

$$G(k) = \tfrac{1}{3}\chi^{-3}\epsilon_\theta k^{-4}E(k), \tag{6}$$

so that a normalization of simulation results for $G(k)$ by $E(k)$ can prevent small deviations of $E(k)$ from an inertial range spectrum from being of consequence.

In an attempt to determine the physical inertial–conductive subrange, CCR also performed a large-eddy simula-

 0899-8213/91/051164-05$02.00  

tion of this subrange. To simulate an inertial velocity field, they artificially forced the turbulence and employed an eddy viscosity subgrid model. An approximate inertial–conductive subrange of the form given by Eq. (6) was observed by CCR for wave numbers much greater than the Corrsin–Obukhov wave number

$$k_{C\text{-}O} = (\epsilon/\chi^3)^{1/4}, \tag{7}$$

but with a proportionality constant slightly larger than $\frac{1}{3}$. This slightly larger value was attributed to the development of higher-order correlations in the velocity field.

## II. LARGE-EDDY SIMULATION

In this paper, we improve upon the CCR large-eddy simulation by performing freely decaying and forced large-eddy simulations of passive temperature fields over a wider range of dimensionless wave numbers $k/k_{C\text{-}O}$. We use the Rogallo code[3] for homogeneous turbulence, modified to include a subgrid model consisting of an eddy-damping term and stochastic force, described in detail elsewhere.[4] In the simulations, the kinematic viscosity of the fluid is assumed to be negligible, i.e., the viscous subrange is not resolved. However, the thermometric conductivities of the simulated temperature fields are chosen so that the conductive scales of the temperature fluctuations are well resolved. An obvious advantage of this type of simulation is that the temperature fluctuations are not directly affected by a subgrid scale model; however, the temperature fluctuations must be indirectly affected by the subgrid model through the nonlinear coupling of $\theta$ to $\mathbf{u}$. Furthermore, any physics that requires a resolved viscous subrange will be absent. In particular, the exponential tail of the viscous–conductive subrange does not appear in our simulation. This subrange, however, has been observed in a direct numerical simulation of the velocity and temperature fields, where both the viscous and conductive scales were resolved.[5]

### A. Freely decaying turbulence

The numerical simulation of freely decaying velocity and temperature fluctuations closely models the decay of turbulent fluctuations created by passing a uniform stream of fluid past a heated grid, and thus has a firm physical basis. We begin the computation by performing a $64^3$ numerical simulation of four different passive temperature fields convected by the same velocity field. The initial energy spectrum of the velocity fluctuations is chosen to be

$$E(k,0) = (256/35)(2/\pi)^{1/2} k_p^{-1} (k/k_p)^8 \times u_0^2 \exp[-2(k/k_p)^2], \tag{8}$$

whereas the initial temperature spectra are all chosen to be $G(k,0) = 2\theta_0^2/u_0^2\ E(k,0)$, where $u_0 = 1$, $\theta_0 = 1$, and $k_p = 5$. The conductivities of the four temperature fields are chosen to be $\chi = 0.03$, 0.07, 0.20, and 0.50. The Prandtl numbers associated with each value of $\chi$ cannot be determined since the viscous scales are unresolved, but they are in any case, much less than one. The time evolution of the energy spectrum is presented in Fig. 1, while the time evolutions of the four temperature spectra are presented in Fig. 2. An inertial subrange energy spectrum is observed to develop.

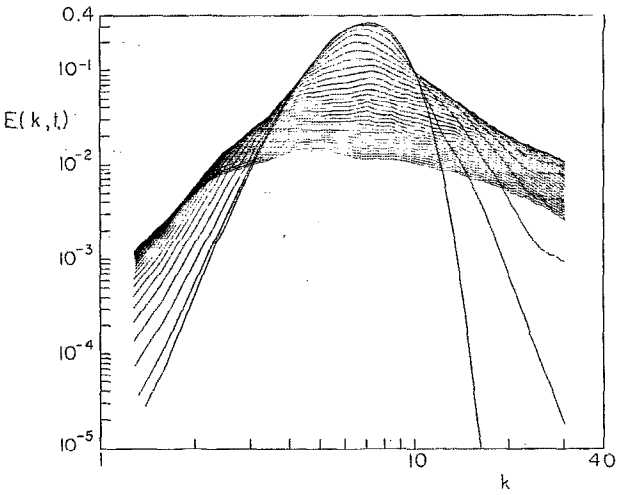


FIG. 1. Time evolution of the energy spectrum for freely decaying turbulence.

After completing the simulation presented in Figs. 1 and 2, we increased the conductivities of the four temperature fields to $\chi = 1.3$, 3.2, 8.0, 20.0, and further time-evolved the flow with a smaller time step [so that the time step is less than the smallest conductive time scale $(\chi_m k_m^2)^{-1}$, where $\chi_m$ is the maximum thermometric conductivity, and $k_m$ is the maximum wave number in the simulation]. In Fig. 3(a), we plot the eight resulting functions $\chi^3 k^4 G(k)/[\epsilon_\theta E(k)]$ vs $k/k_{C\text{-}O}$, at the latest time of the flow evolutions. If the BHT result, Eq. (6), is correct, then these plots should, for $k \gg k_{C\text{-}O}$, asymptotically approach the horizontal line drawn at $\frac{1}{3}$. For greater clarity, an enlargement of Fig. 3(a) is presented in Fig. 3(b).

From our simulation data, the BHT result is observed to be approached asymptotically in the far inertial–conductive subrange. The convergence of our results to $\frac{1}{3}$ occurs at a rather large value of $k/k_{C\text{-}O}$, so that the value 0.39 instead of $\frac{1}{3}$ previously observed by CCR is due to their simulation of a temperature field with insufficiently large values of $k/k_{C\text{-}O}$.

### B. Forced turbulence

A more precise determination of the temperature spectrum in the near and far inertial–conductive subrange is possible if the velocity and temperature fluctuations are forced so as to obtain a statistically stationary state. A time average over the steady state can then be performed yielding a better statistical sample. The velocity fluctuations are forced by keeping the amplitudes of the lowest wave-number Fourier components of the velocity field fixed,[4] whereas the temperature fluctuations are forced by imposing a uniform mean temperature gradient. The simulation is begun with a fully developed velocity field, and an absence of temperature fluctuations. The velocity fluctuations then create temperature fluctuations from the mean temperature gradient. The velocity and temperature fields are time-advanced until the temperature fluctuations reach a statistically stationary state, after which statistics of the fields are time-averaged until they converge.

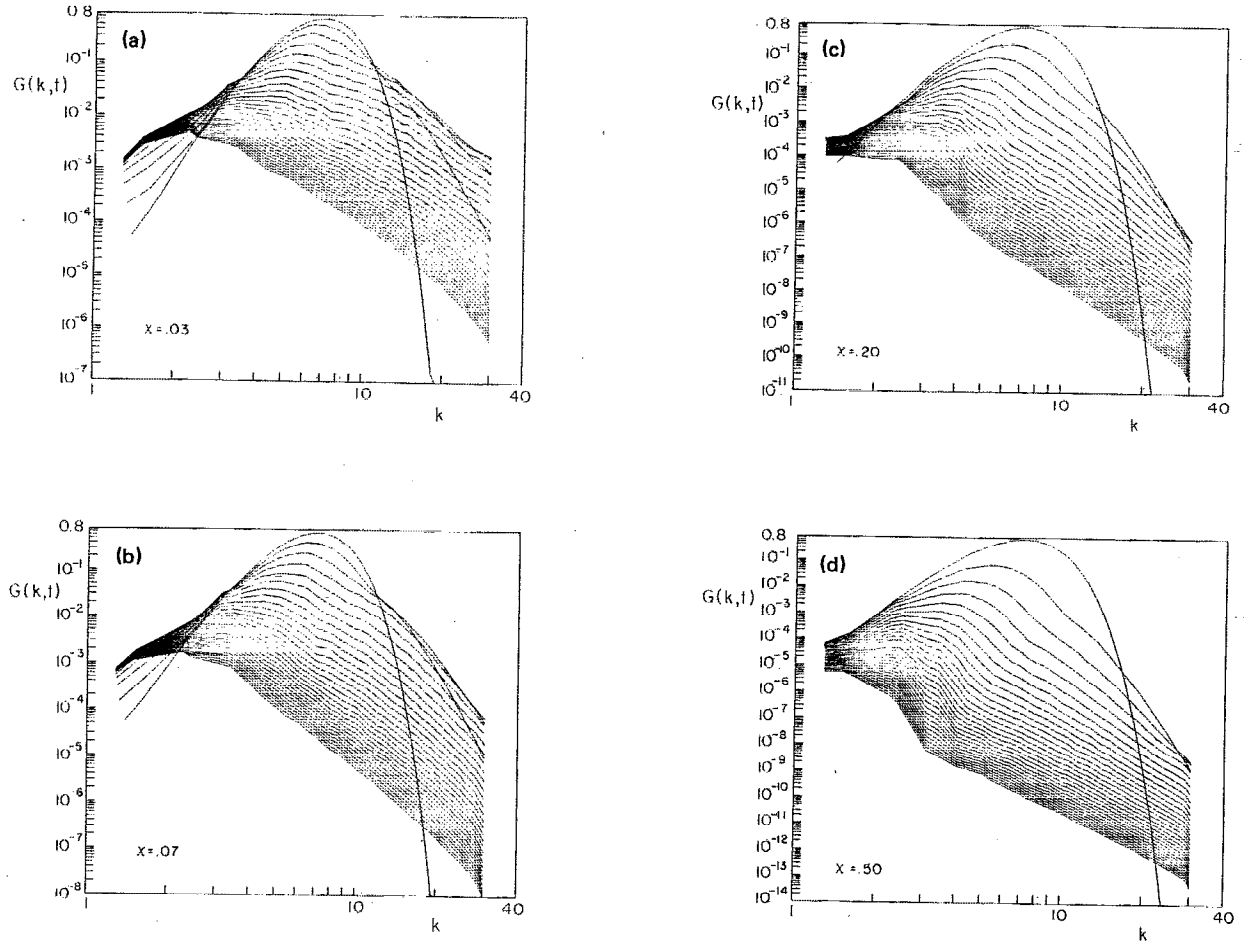


FIG. 2. Time evolution of the temperature spectrum for freely decaying turbulence. (a) $\chi = 0.03$; (b) $\chi = 0.07$; (c) $\chi = 0.20$; (d) $\chi = 0.50$.

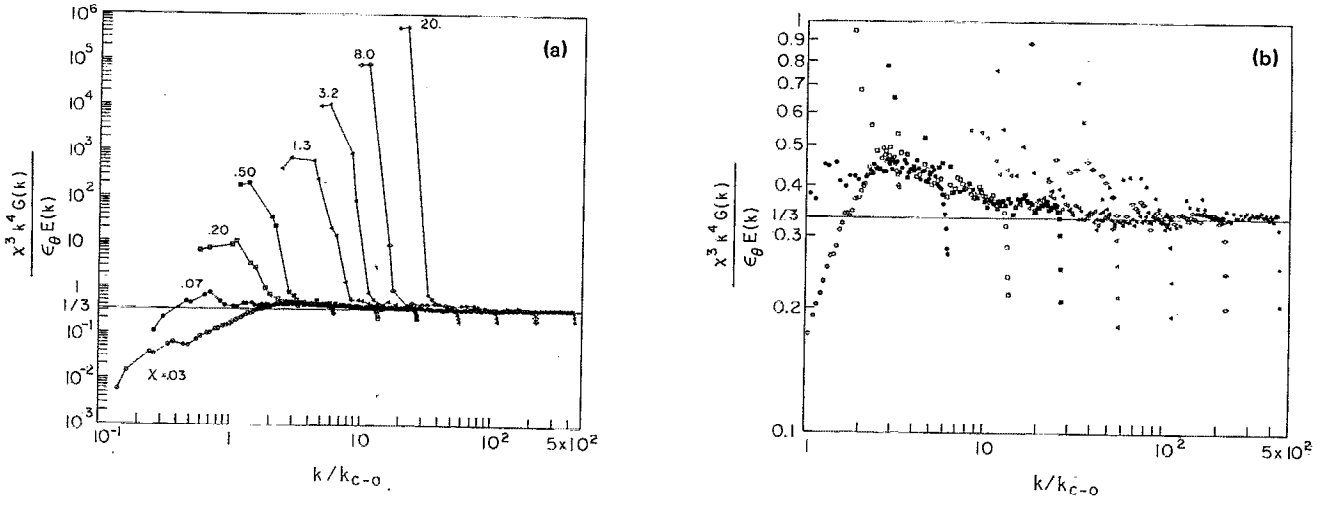


FIG. 3. Spectrum of $\chi^3 k^4 G(k)/[\epsilon_\theta E(k)]$ vs $k/k_{c\text{-}o}$ for eight different temperature fields for freely decaying turbulence. The horizontal line is the BHT result. (a) Full spectrum; (b) inertial–conductive subrange.

The externally imposed uniform mean temperature gradient contributes directly to the flux of $\theta^2$ through wave number $k$, and consequently, must be included when computing $\epsilon_\theta$. By equating the constant flux of $\theta^2$ through wave number $k$ when conductive effects are negligible to the total conductive dissipation rate, we find that $\epsilon_\theta$ is now equal to

$$\epsilon_\theta = 2\chi\left(\beta^2 + \int_0^\infty k^2 G(k)dk\right), \tag{9}$$

where $G(k)$ is the spectrum of the fluctuating temperature field (excluding the mean), and

$$\beta = -\frac{d\bar{T}}{dz} \tag{10}$$

is the uniform mean temperature gradient that we impose in the $z$ direction. For convenience, we have taken $\beta = 1$, although any nonzero value will suffice since $\beta$ only sets the relative scale of the temperature fluctuations.

In Fig. 4, we plot the time average of the energy spectrum $E(k)$ vs $k$ in computational units obtained from a $64^3$ numerical simulation of the forced velocity field. A reasonable $k^{-5/3}$ spectrum is observed over most of the computational domain. In Fig. 5, we plot the time average of $\chi^3 k^4 G(k)/[\epsilon_\theta E(k)]$ vs $k/k_{C\text{-}O}$ for 11 temperature fields of different conductivities generated by the simulated velocity field acting on a uniform mean temperature gradient. The results agree qualitatively with those from the freely decaying simulations, with the statistical scatter greatly reduced because of the time averaging.

Figure 5 determines the temperature spectrum in both the near and far inertial–conductive subrange. The behavior of the spectrum in the far subrange ($k/k_{C\text{-}O} \gtrsim 80$) is well predicted by the BHT value of $\frac{1}{3}$ whereas there are significant departures from this value in the near subrange ($3 \lesssim k/k_{C\text{-}O} \lesssim 80$). This deviation is to be expected since the BHT analysis depends on $k/k_{C\text{-}O}$ being much greater than unity. What we have done is extended the BHT analytical result numerically to values of $k/k_{C\text{-}O}$ of order unity.

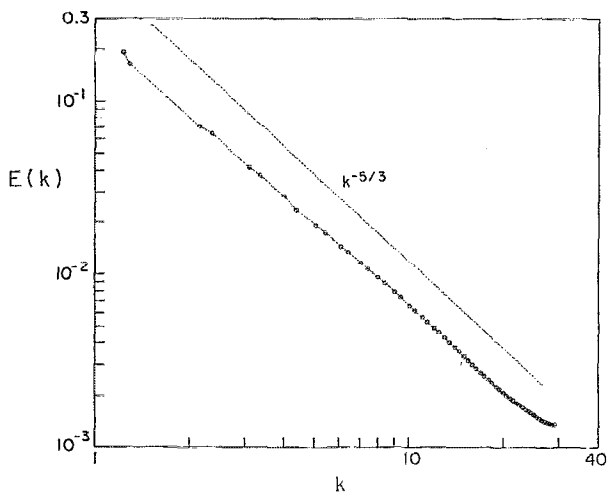


FIG. 4. Time average of the energy spectrum $E(k)$ for forced turbulence.

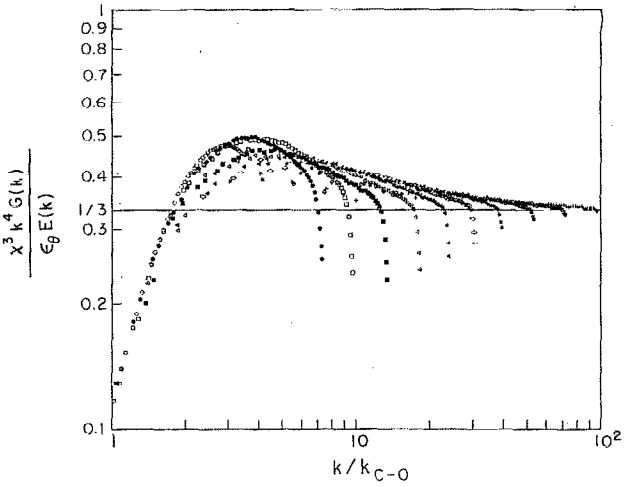


FIG. 5. Time average of the inertial–conductive subrange spectrum of $\chi^3 k^4 G(k)/[\epsilon_\theta E(k)]$ vs $k/k_{C\text{-}O}$ for 11 different temperature fields for forced turbulence.

However, there is another important difference between the results of Fig. 5 and those of BHT. If one assumes (as is implied by the BHT analysis) that the only statistical quantities that characterize the temperature spectrum in the inertial subrange are the cascade rates $\epsilon$ and $\epsilon_\theta$, and the Corrsin–Obukhov length scale $k_{C\text{-}O}^{-1}$, then dimensional analysis requires the simulation results displayed in Fig. 5 to collapse to a single universal curve. However, small but significant departures from this universal scaling in the near inertial–conductive subrange can be observed. We expect these deviations to be of two kinds: real physical ones, and those that are purely numerical. Numerical errors are clearly evident at the largest computational wave numbers of each simulation and may be attributed to a finite truncation of the Fourier series representing the velocity and temperature fields. In addition, some of the scatter at the smallest computational wave numbers can be attributed to poor statistical sample at these wave numbers. The forcing and subgrid modeling of the velocity field may result in other unknown numerical errors, primarily affecting the spectra at the smallest and largest computational wave numbers, respectively. Yet the systematic deviations of the temperature spectra from a universal curve at intermediate computational wave numbers, where the simulation statistics are the most reliable, suggest that a real physical mechanism may be responsible. An intriguing possibility for this mechanism that has been widely discussed in the literature is intermittency. An analysis of an intermittency correction to the inertial–conductive subrange has been performed by Van Atta[6] using a bivariate lognormal distribution for the local temperature and velocity dissipation rates. His results indicate a small correction to the $k^{-4}$ power law appearing in Eq. (6) due to a cross correlation between these dissipation rates.

In conclusion, the BHT analytical result for the far inertial–conductive subrange has been extended by means of a numerical simulation to the near part of this subrange. In addition, small but significant deviations from a universal

scaling law based on Corrsin–Obukhov units have been observed. A determination of the precise causes of these deviations will require careful future analysis.

## ACKNOWLEDGMENTS

The author gratefully acknowledges the help and guidance of Dr. V. M. Canuto and Dr. R. S. Rogallo. The author also thanks Dr. G. J. Hartke and Mr. O. Schilling for their useful discussions. The simulations of forced turbulence were begun during the 1990 Center for Turbulence Research Summer Program, in collaboration with Dr. M. M. Rogers, Dr. R. S. Rogallo, and Professor C. H. Gibson.

This research was partially supported by NASA Ames, which generously provided the computer facilities for these computations. This paper was written while the author held a National Research Council–NASA GISS Research Associateship.

[1] J. Chasnov, V. M. Canuto, and R. S. Rogallo, Phys. Fluids **31**, 2065 (1988).
[2] G. K. Batchelor, I. D. Howells, and A. Townsend, J. Fluid Mech. **5**, 134 (1959).
[3] R. S. Rogallo, NASA Tech. Memo. 81315, 1981.
[4] J. R. Chasnov, Phys. Fluids A **3**, 188 (1991).
[5] R. M. Kerr, J. Fluid Mech. **211**, 309 (1990).
[6] C. W. Van Atta, Izv. Atmos. Oceanic Phys. **10**, 712 (1974).